Optical Measurement and Control of Spin Diffusion in *n*-Doped GaAs Quantum Wells

S. G. Carter,[1] Z. Chen,[1,2] and S. T. Cundiff[1]

[1]*JILA, National Institute of Standards and Technology and University of Colorado, Boulder, Colorado 80309-0440, USA*
[2]*Department of Physics, University of Colorado, Boulder, Colorado 80309-0390, USA*

(Received 17 July 2006; published 26 September 2006)

Transient spin gratings are used to study spin diffusion in lightly *n*-doped GaAs quantum wells at low temperatures. The spin grating is shown to form in the excess electrons from doping, providing spin relaxation and transport properties of the carriers most relevant to spintronic applications. We demonstrate that spin diffusion of the these carriers is accelerated by increasing the density or energy of the optically excited carriers. These results can be used to better understand and even control spin transport in experiments that optically excite spin-polarized carriers.

DOI: 10.1103/PhysRevLett.97.136602 PACS numbers: 72.25.Fe, 72.25.Dc, 75.40.Gb, 78.47.+p

In spintronic devices, spin-polarized carriers must be transferred from one point to another with little loss of spin polarization. This requires a reasonably long spin relaxation time (τ_s) and reasonably fast transport of the spins. Long spin relaxation times (from nanoseconds to microseconds) have been measured in bulk semiconductors [1] and semiconductor quantum wells [2,3] (QWs), typically at low temperatures. Spin transport in semiconductors has been studied by injecting spin-polarized carriers (either optically or with ferromagnetic contacts) and imaging the spin polarization with Kerr microscopy [4,5]. The transport properties are determined by two related quantities, the spin mobility μ_s and the spin diffusion coefficient D_s. The drift velocity of spin packets in response to an electric field is determined by μ_s while D_s determines how rapidly spin packets spread out.

The spin transport properties have often been assumed to be the same as the charge transport properties, but recent results demonstrate that D_s is reduced due to Coulomb interactions [6,7]. This reduction modifies the relationship between D and μ, which is often described by the Einstein relation in nondegenerate samples, $eD = \mu kT$. In lightly doped bulk GaAs samples at 1.6–4 K, D_s and μ_s have been measured as $\sim 10\ \mathrm{cm}^2/\mathrm{s}$ and $2\text{–}3 \times 10^3\ \mathrm{cm}^2/\mathrm{V\,s}$, respectively [4,5]. This value of D_s is an order of magnitude higher than expected from the Einstein relation and seems to contradict the reduction of D_s due to the Coulomb interaction. While the high value in D_s may be explained by degeneracy of the electrons [8], which also modify the Einstein relation, spin transport properties are still an area of active discussion [9–11]. These deviations of D_s from expected behavior illustrate the importance of understanding other influences on spin transport. This Letter demonstrates that D_s is strongly affected by the optical excitation conditions and contrasts the diffusion properties of optically excited carriers and excess electrons from doping.

There have been several experiments on spin diffusion in undoped quantum wells [12–14] and more recently in heavily *n*-doped quantum wells [7] using transient spin gratings. In this method, two optical pulses (pumps) with identical energies near the band gap are coincident on the sample from different directions, exciting electron-hole pairs. For collinearly polarized pumps, interference modulates the intensity across the excitation spot, generating a grating in the concentration of optically excited carriers. The grating period is determined by the angle between the pump beams. For cross-linearly polarized pumps, the net polarization alternates between right and left circular polarization across the excitation spot. Because of interband selection rules, this generates carriers with alternating spin polarization but a uniform total concentration. A delayed probe pulse is diffracted off of the grating, giving the grating amplitude as a function of time. For a concentration or spin grating, the polarization of the diffracted beam is parallel or perpendicular to that of the probe, respectively. The concentration grating (CG) decays due to carrier recombination and spatial diffusion, while the spin grating (SG) decays due to spin relaxation and spin diffusion. The effects of relaxation and diffusion can be separated by varying the grating period, as will be discussed below.

In the previous SG measurements of undoped and heavily doped QW samples, τ_s was relatively short (<100 ps), giving limited application for spintronics devices. In this Letter, we examine spin diffusion in lightly *n*-doped ($2 \times 10^{10}\ \mathrm{cm}^{-2}$) QWs at low temperatures, with a τ_s of several nanoseconds. Such lightly doped samples have received much attention for spintronic devices because of their long values of τ_s. We measure spin diffusion and relaxation under a variety of conditions, systematically varying the excitation density, excitation photon energy, and temperature. The results demonstrate that increasing the excitation intensity and excitation energy increases D_s. This dependence is very important for the many studies of spin dynamics that optically generate a spin polarization and may help reconcile differences between experimental data and theoretical predictions. Comparison of SGs to CGs also demonstrates significantly slower spin diffusion of excess electrons than diffusion of the unpolarized optically excited carriers.

The sample consists of 10 periods of coupled GaAs QWs, with silicon modulation doping centered in the 41 nm $Al_{0.3}Ga_{0.7}As$ barriers. The coupled QWs are

10 nm and 12 nm with a 2.5 nm $Al_{0.2}Ga_{0.8}As$ tunnel barrier. The wells are strongly coupled, with the lowest electron wave function extending into both wells, while the lowest heavy-hole state is primarily confined to the wider well. Coupled QWs are not necessary for these experiments, and we expect no qualitative differences in the spin properties when comparing to single QWs. The doping was designed to give 2×10^{10} electrons/cm^2 per well (n_{dop}). A 30 period $AlAs/Al_{0.3}Ga_{0.7}As$ Distributed Bragg reflector (DBR) grown beneath the QWs acts as a mirror, so reflected light is transmitted twice through the QW stack. The sample was mounted in a superconducting magnet cryostat with the magnetic field in the QW plane (Voigt geometry). The reflectivity at 4 K is displayed in Fig. 1(a), with the exciton and trion (negatively charged exciton) resonances labeled.

The laser pulses are generated by a mode-locked Ti:sapphire laser, with the wavelength typically set to 804.5 nm (1.541 eV) and a spectral bandwidth of 3.0 nm (5.7 meV). The laser bandwidth covers both the exciton and trion resonances [Fig. 1(a)]. For some experiments, the pump pulses (labeled A and B) pass through a pulse shaper which spectrally filters the pump spectrum to 0.5 nm (1 meV). Intensity cross-correlation measurements are used to ensure that the pump pulses are temporally coincident and give the duration of the unfiltered and filtered pulses as 260 fs and 2.5 ps, respectively.

The beams are focused on the sample in a so-called box geometry, as shown in Fig. 1(b), with diameters at the focus of 150 μm for pump A, 100 μm for pump B, and 60 μm for the probe. The angle between the pumps is varied between 4° and 9°, giving grating periods from 5 μm to 11 μm. The reflected beams are also at three corners of a rectangle, with the diffracted signal at the fourth corner of the rectangle ($-\vec{k}_A + \vec{k}_B + \vec{k}_C$ before reflection). For collinear experiments, both pumps (A and B) are polarized horizontally, while for cross-linear experiments, pump A is horizontal and pump B is vertical. The probe is vertically polarized, and the diffracted beam passes through a linear polarizer oriented vertically (horizontally) for the collinear (cross-linear) case. The diffracted beam is detected by an amplified photodiode.

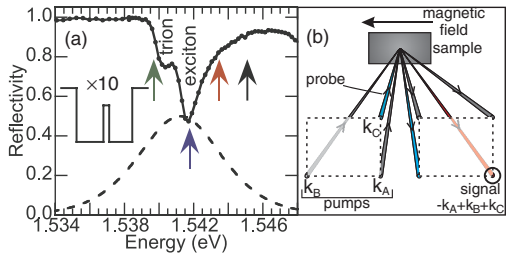

FIG. 1 (color online). (a) Reflectivity (solid, black line) of the doped quantum well (QW) sample at ~4 K and a typical unfiltered laser spectrum (dashed line). The arrows represent the filtered pump energies used. The QW profile is inset in the figure. (b) Geometry of the three-beam four-wave mixing.

Figure 2(a) displays the diffracted signal from SGs and CGs for an undoped reference sample, identical to the doped sample previously described but with no modulation doping of the coupled QWs. The CG signal intensity decays with a time constant $T_c/2$ of 143 ps. We attribute this decay time T_c to the recombination and diffusion of the optically excited carriers. The signal decays to a value of ~0.01 at long delays. Such offsets are common and may be due to a thermal grating.

In the undoped sample, the SG amplitude sharply decreases away from zero delay, making it an order of magnitude weaker than the CG after ~10 ps. The SG signal oscillates at 30.5 GHz, due to precession of the SG in the 4 T magnetic field. The presence of the magnetic field is not essential, but a field is typically used to monitor changes in the precession frequency and to isolate the signal due to spins. Within experimental error, the magnetic field has no effect on the spin diffusion of the doped sample (up to 4 T) but it does decrease τ_s. After excitation, the SG is initially oriented perpendicular to the QW plane and the in-plane magnetic field [see Fig. 2(a)]. As the SG precesses about the magnetic field, the diffracted field oscillates at the Larmor precession frequency, and the diffracted intensity oscillates at twice this frequency. The SG primarily consists of one component that decays with a time constant of ~150 ps, which we attribute to the spin of the optically excited electrons. Hole spin lifetimes are assumed to be much shorter. A second weaker component has a longer time constant of ~1–2 ns, which we attribute to a small number of electron spins in the wells from unintentional doping.

In the doped sample [Fig. 2(b)], the CG looks similar to that for the undoped sample, but the decay is not a single

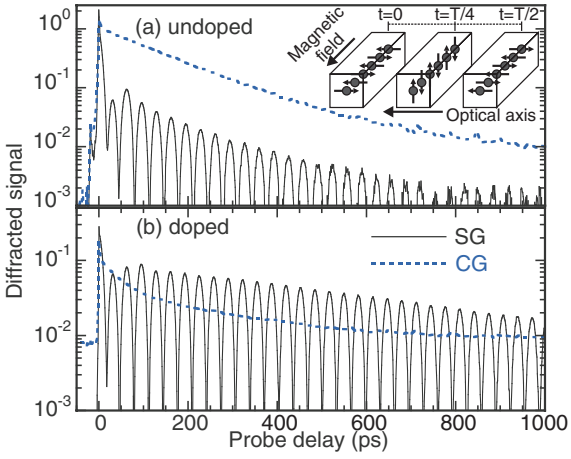

FIG. 2 (color online). Transient gratings on (a) the undoped and (b) the doped samples at a magnetic field of 4 T, showing the spin gratings (SGs) and the concentration gratings (CGs). The vertical scale is logarithmic. The pumps (unfiltered) and probe are resonant with the exciton or trion states, giving an excitation density of 3.7×10^9 cm^{-2} (6.6×10^9 cm^{-2}) for the doped (undoped) sample. Diagrams of the spin grating are inset in (a) at several times, illustrating precession of the grating.

exponential, and there is a negative delay signal. The negative delay signal may be due to a very long-lived grating in the lattice temperature that lasts longer than the laser repetition period (13 ns). This curve can be fitted to the square of the sum of two exponentials with an offset, giving decay times of 47 ps and 490 ps. Multiple decay times are not surprising since the pump excites both excitons and trions, perhaps with varying lifetimes and degrees of localization. Because of these complications, few results on CGs will be presented here.

In contrast with the undoped sample, the SG amplitude in the doped sample is comparable to the CG amplitude. This difference indicates a change in the source of nonlinearity in going from undoped to doped. After the first 100 ps, the SG decays with a time constant of 1.10 ns. This time constant is longer than the lifetime of optically excited carriers and indicates that the SG is transferred to the excess electrons present from doping. The initial rise in the SG amplitude in the first 100 ps (after the zero-delay spike) appears to be due to an interference between the excess electron SG and either the optically excited electron or hole spins. The first 40–220 ps are excluded from the fits for this reason. The fitting function is $A[\cos(2\pi ft + \phi) \times \exp(-\Gamma t)]^2$, where A is the amplitude, f is the precession frequency, ϕ is the initial phase, and Γ is the grating decay rate.

In the diffusive regime, SGs will decay according to $\Gamma = D_s q^2 + 1/\tau_s$, where q is the grating wave vector and τ_s is the spin lifetime. To separate the effects of diffusion and relaxation, the grating decay rate is measured as a function of q by varying the angle θ between the two pumps. In Fig. 3, the grating decay rate is plotted versus q^2 for a series of (a) excitation densities and (b) temperatures. The data in (a) were taken at 4 K, and the data in (b) were taken at an excitation density (n_{ex}) of 3.7×10^9 cm^{-2}. Each set of data points is linear, with the slope giving D_s and the intercept on the Γ axis giving $1/\tau_s$. Table I displays the values of τ_s and D_s obtained from linear fits of the data. Going from $n_{ex} \ll n_{dop}$ to $n_{ex} > n_{dop}$, D_s goes from about 5 to 11 cm^2/s. The value of τ_s decreases as well. As the temperature is increased from 4 K, a similar trend is observed, with D_s reaching 17 cm^2/s at 20 K. However, as seen in the insets of Fig. 3, the spin precession frequency increases by 0.7% with n_{ex} while the frequency decreases by 3.7% with temperature. This difference indicates that increasing the excitation density does not simply heat up the crystal lattice.

SGs were also measured for a series of pump photon energies, as displayed in Fig. 4(a). The spectrally filtered pumps were set to four different energies, from the lower edge of the trion to 3.3 meV above the exciton [15]. (See the arrows in Fig. 1.) The probe was not spectrally filtered and covered both the exciton and trion. The pump power was adjusted at each energy to keep n_{ex} roughly constant at 1.1×10^{10} cm^{-2}. However, only a density of roughly 0.6×10^{10} cm^{-2} could be obtained at 1.5451 eV, due to the weak absorption. The spin diffusion coefficient increases from ~4 cm^2/s to ~7.5 cm^2/s when pumping a few meV above the exciton resonance. This result is surprising since the SG signal comes primarily from the excess electrons, which should be independent of the energy of the optically excited carriers, particularly after recombination. One interesting fact is that fits to the SG signal are not very good at times greater than ~1 ns, giving a smaller amplitude than is measured. When only times greater than 750 ps are fitted, D_s decreases to 5 or 6 cm^2/s for the pump energies above the exciton, indicating there is a change in D_s as a function of time. Also, when pumping

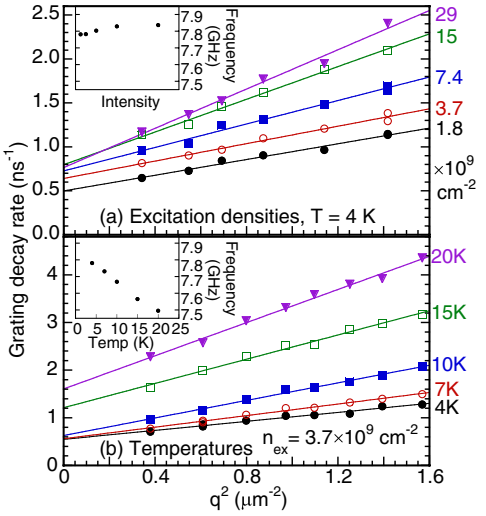

FIG. 3 (color online). SG decay rate of the doped sample at 2 T as a function of q^2 for a series of (a) excitation densities and (b) temperatures. The pump and probe were not spectrally filtered. In part (a), taken at 4 K, the data are labeled by n_{ex}, and in part (b), the data are labeled by temperature. The solid lines are linear fits. The inset graphs plot the average precession frequency as a function of (a) excitation density and (b) temperatures.

TABLE I. Lifetimes (τ) and diffusion coefficients (D) obtained from linear fits to the data plotted in Fig. 3 and 4. Twice the standard error obtained from fitting is given in parentheses. The subscript s denotes SG, and the subscript c denotes CG.

n_{ex} ($\times 10^9$ cm^{-2})	τ_s (ns)	D_s (cm^2/s)	Temperature (K)	τ_s (ns)	D_s (cm^2/s)
1.8	2.0 (0.2)	4.5 (0.5)	4	1.8 (0.2)	4.7 (0.6)
3.7	1.6 (0.2)	4.9 (0.6)	7	1.8 (0.2)	6.1 (0.5)
7.4	1.4 (0.1)	6.7 (0.8)	10	1.6 (0.2)	9.2 (0.7)
15	1.3 (0.1)	9.3 (0.8)	15	0.8 (0.1)	12.7 (1.1)
29	1.3 (0.2)	11.2 (1.3)	20	0.6 (0.1)	17.4 (1.3)
Pump energy (eV)	τ_s (ns)	D_s (cm^2/s)		τ_c (ps)	D_c (cm^2/s)
1.5451	2.2 (0.2)	7.4 (0.4)		478 (72)	33 (3.3)
1.5435	2.0 (0.1)	7.7 (0.3)		322 (24)	28 (2.5)
1.5418	2.0 (0.3)	5.6 (0.8)		176 (10)	22 (3.6)
1.5397	1.8 (0.1)	4.2 (0.2)		43 (1.4)	7.7 (7.8)

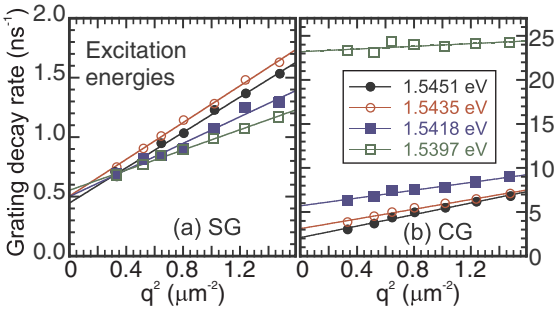

FIG. 4 (color online). (a) SG and (b) CG decay rates of the doped sample at 4 K and 2 T as a function of q^2 for a series of pump photon energies (filtered). The solid lines are linear fits.

at the exciton, there is a weaker amplitude signal of higher precession frequency that appears to have a negligible D_s.

Figure 4(b) displays CG results for the same series of pump energies. Because of the previously mentioned difficulties in fitting the CG decay, the rates plotted are obtained by calculating the time interval over which the signal decays to $1/e$ times its initial value (taken at $\sim$20 ps to eliminate any initial spikes in the signal). The diffusion coefficient D_c is about 30 cm^2/s when pumping above the exciton energy but decreases to a much smaller value when pumping at the trion. The lifetime τ_c varies a great deal as well, indicating multiple carrier lifetimes and degrees of localization.

The influence of excitation conditions on exciton lifetimes [16,17] and localization [18,19] is well known. The mechanism for affecting excess electrons in a doped QW is not as clear. Based on the different dependences of the precession frequency on excitation density and temperature, increasing the pump intensity does not significantly heat the lattice. Instead, we hypothesize that high intensity pumping increases the electron temperature, freeing electrons from localization sites. In lightly modulation-doped QWs at low temperature, electrons are localized by the remote ionized donors [20]. This localization probably explains why spin diffusion of the excess electrons is typically much smaller than diffusion of the unpolarized neutral excitons. Spin Coulomb drag may also play a role [6,7]. Increasing the electron temperature should allow easier movement of electrons between localization sites, thus increasing D_s. Heating of the excess electrons should occur due to relaxation of high-energy optically excited carriers down to the trion state. This temperature should slowly decrease as heat is transferred to the lattice. The increase in D_s with excitation energy is consistent with this theory as is the aforementioned observation of D_s decreasing with time.

We have performed a systematic study of spin diffusion of excess electrons in a doped QW sample. The fact that the excess electrons are measured is demonstrated by the long SG decay times, which are typically longer than the optically excited carrier lifetime. The large variation of the optically excited CG properties compared to the SG properties [see Fig. 4] also indicates that the SG signal is dominated by a single component—the excess electrons. Sensitivity to these electrons is important for spintronic applications since they have long-lived spin lifetimes and can be used to transport spin information. Furthermore, the contrast between diffusion of the excess electrons and the optically excited carriers is pertinent to many optical studies of semiconductor transport. Most importantly, we demonstrate that spin diffusion of the excess electrons is accelerated by increasing the excitation density and excitation energy. This acceleration is consistent with a heating of the excess electrons due to relaxation of energetic optically excited carriers. These results are particularly relevant for understanding spin transport studies that use optical spin injection or detection. This effect may even be used to control spin transport by varying the excitation conditions.

We thank Andrew S. Huntington and Larry A. Coldren at the University of California, Santa Barbara, for providing our samples, and we acknowledge support from the NSF. S. G. Carter is supported by the National Research Council.

[1] J. M. Kikkawa and D. D. Awschalom, Phys. Rev. Lett. **80**, 4313 (1998).
[2] J. M. Kikkawa *et al.*, Science **277**, 1284 (1997).
[3] A. M. Tyryshkin *et al.*, Phys. Rev. Lett. **94**, 126802 (2005).
[4] J. M. Kikkawa and D. D. Awschalom, Nature (London) **397**, 139 (1999).
[5] S. A. Crooker *et al.*, Science **309**, 2191 (2005).
[6] I. D'Amico and G. Vignale, Europhys. Lett. **55**, 566 (2001).
[7] C. P. Weber *et al.*, Nature (London) **437**, 1330 (2005).
[8] M. E. Flatte and J. M. Byers, Phys. Rev. Lett. **84**, 4220 (2000).
[9] L. Jiang *et al.*, J. Appl. Phys. **98**, 113702 (2005).
[10] A. Punnoose and A. M. Finkel'stein, Phys. Rev. Lett. **96**, 057202 (2006).
[11] M. Hruska *et al.*, Phys. Rev. B **73**, 075306 (2006).
[12] A. R. Cameron, P. Riblet, and A. Miller, Phys. Rev. Lett. **76**, 4793 (1996).
[13] S. Adachi *et al.*, Opt. Commun. **174**, 291 (2000).
[14] K. Jarasiunas *et al.*, Appl. Phys. Lett. **84**, 1043 (2004).
[15] For these measurements, the reflectivity spectrum had shifted up 3 meV relative to the spectrum shown in Fig. 1, perhaps due to strain or electric field. The shift did not seem to alter the diffusion or relaxation properties, but the precession frequency decreased by several percent. The pump energies listed here have been shifted down to match the spectral features in Fig. 1.
[16] R. Eccleston *et al.*, Phys. Rev. B **45**, 11 403 (1992).
[17] J. I. Kusano *et al.*, Phys. Rev. B **40**, 1685 (1989).
[18] J. Hegarty, L. Goldner, and M. D. Sturge, Phys. Rev. B **30**, 7346 (1984).
[19] M. T. Portella-Oberli *et al.*, Phys. Rev. B **66**, 155305 (2002).
[20] G. Finkelstein, H. Shtrikman, and I. Bar-Joseph, Phys. Rev. Lett. **74**, 976 (1995).